



Socially Aware Robot Navigation System in Human-populated and Interactive Environments based on an Adaptive Spatial Density Function and Space Affordances

Araceli Vega^a, Luis J. Manso^{a,b}, Douglas G. Macharet^c, Pablo Bustos^a, Pedro Núñez^a

^a*RoboLab, Universidad de Extremadura, Cáceres, Spain <http://roboLab.unex.es>*

^b*School of Engineering and Applied Science, Aston University, Birmingham, United Kingdom*

^c*VeRLab, Universidade Federal de Minas Gerais, Belo Horizonte, Brazil*

ABSTRACT

Traditionally robots are mostly known by society due to the wide use of manipulators, which are generally placed in controlled environments such as factories. However, with the advances in the area of mobile robotics, they are increasingly inserted into social contexts, i.e., in the presence of people. The adoption of *socially acceptable behaviours* demands a trade-off between social comfort and other metrics of efficiency. For navigation tasks, for example, humans must be differentiated from other ordinary objects in the scene. In this work, we propose a novel human-aware navigation strategy built upon the use of an adaptive spatial density function that efficiently cluster groups of people according to their spatial arrangement. Space affordances are also used for defining potential *activity spaces* considering the objects in the scene. The proposed function defines regions where navigation is either discouraged or forbidden. To implement a socially acceptable navigation, the navigation architecture combines a probabilistic roadmap and rapidly-exploring random tree path planners, and an adaptation of the elastic band algorithm. Trials in real and simulated environments carried out demonstrate that the use of the clustering algorithm and social rules in the navigation architecture do not hinder the navigation performance.

© 2018 Elsevier Ltd. All rights reserved.

1. Introduction

The use of mobile robots in social contexts is expected to grow in the years to come. Efforts are being made to enable them to perform routine tasks in environments such as homes, offices, hospitals, and museums. A fundamental characteristic of these environments is the presence of humans, which forces robots to consider them in a special way, for example, during navigation.

The concept of *socially acceptable navigation* has gained attention recently, especially in the context of the study of Human-Robot Interaction (HRI). More specifically, when considering the path planning problem in human-populated environments, the constraints imposed by social conventions must be respected, turning them into *anthropomorphic paths* (Scandolo and Fraichard, 2011). In this respect, research on social robot navigation has followed different goals, crosses many domains

and calls for inquiries such as: Can the robot make speak now? Can the robot pass at that distance from the person? How fast can the robot move without disturbing people's sense of safety? Most interaction situations between humans and robots consider the case where the robot must perform a task (e.g. navigate) while reducing the possible social impact.

Previous authors' work proposed a social path planner which includes a model of social navigation (Núñez et al., 2016). In (Vega et al., 2017a), (Vega et al., 2017b) the authors present an algorithm for human-centered navigation, where they define a method for clustering groups of people in the robot's surrounding based on a density function. The paper at hand extends these works, and it is focused on a path-planning strategy where it is assumed that humans do not want to interact with the robot but with other humans and objects in the scene. A mathematical model built upon the use of an adaptive density function in order to efficiently cluster the individuals is described. The

clustering algorithm analyzes the environment and then clusters the individuals into groups according to social interactions between them. The adaptive spatial density function models the personal space around groups of people, which prevents the emotional discomfort humans may feel when approached closer than they like. The concept of personal space is related to non-verbal social rules, generally referred as *proxemics* (Hall, 1966), which defines spaces that humans mutually respect during an interaction.

As novelty, in this paper, it is also included the concept of *space affordances*, which refers to spaces where humans usually perform particular activities (Rios-Martinez, 2013). In interactive scenarios, these spaces are related to objects with which humans often interact, for example, the space near a poster.

Finally, the system adapts the navigation architecture for considering both the personal spaces and the space affordances, where navigation is either discouraged or forbidden. Figure 1 illustrates the problem to solve: the robot located in the kitchen has to take the best route from its current pose to the living-room (target) along with a complex environment with people while minimizing the level of discomfort in humans.

In summary, the **main contributions** of the presented work are: i) an adaptive spatial density function that allows clustering people in the environment; ii) an extension of the previous social navigation system, which has been also described in this paper; and iii) the inclusion of the space affordances concept in this social navigation system. In particular, this paper significantly extends the work initially presented in (Vega et al., 2017b), including a thorough assessment of the adaptive spatial density function; the application and evaluation of the affordances space for interactive scenarios; the application and evaluation of the social navigation stack to both, real and simulated scenarios, considering a wider set of metrics; and a comparison of the proposed social navigation approach with respect to non human aware navigation system.

The remainder of this paper is organized as follows: in Section 2 we present a review of related work. An overview of the proposed navigation system is described in Section 3. The adaptive spatial density function and space affordances for social mapping are presented in detail in Section 4 and Section 5, respectively. Next, the social navigation architecture is described in Section 6, and validated by a group of experiments on real and simulated human-populated and interactive environments, whose results are shown in Section 7. Finally, in Section 8 we draw the conclusions and discuss avenues for future research.

2. Related works

Usually, robots working in human environments have used navigation algorithms where all obstacles are considered of similar relevance, including people. To avoid discomforting humans, social robots must consider them special entities, evaluating the people' level of comfort with respect to the route of the robot.

Social navigation has been extensively studied in the last decade and several theories and methods have been proposed since then (see (Kruse et al., 2013), (Rios-Martinez et al., 2015) and more recently (Charalampous et al., 2017) for deep reviews). The main idea is to create socially acceptable behaviors

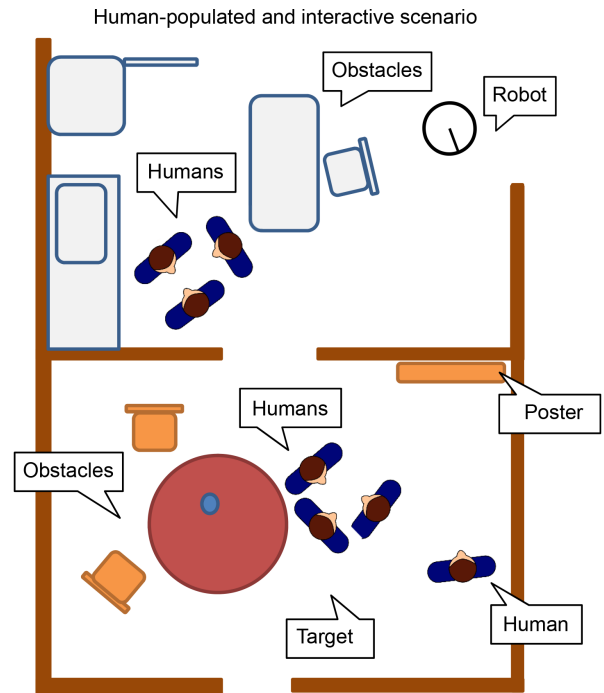


Figure 1: Scenario used to explain the method described in this paper. The robot is operating in a human-populated environment. It has to choose the best route and navigate without causing discomfort to the humans nearby.

for robots during their navigation, what has been introduced as *social mapping* (Charalampous et al., 2016). This social mapping deals with the problem of human-aware robot navigation and considers factors like human comfort, sociability, safety and naturalness (Kruse et al., 2013). More recently, in (Kostavelis, 2017) the concept of *behavioral mapping* has been introduced, where the authors extend social mapping to a behavioral model acting as a mediator that facilitates seamless cooperation among the humans.

Under this prism, different works such as (Mumm and Mutlu, 2011; Walters et al., 2011; Mead and Matarić, 2012), have shown that the same proxemic zones that exist in human-human interaction can also be applied to human-robot interaction scenarios. A broad survey and discussion regarding the social concepts of proxemics theory applied in the context of human-aware autonomous navigation was presented in (Rios-Martinez, 2013; Rios-Martinez et al., 2015). Most of these works define areas where robot navigation is forbidden, that is, when social robots plan to navigate, they must be aware of the permitted and forbidden actions in social spaces (Rios-Martinez et al., 2015). The works presented in (Sisbot et al., 2007; Svenstrup et al., 2009; Kessler et al., 2011; Kruse et al., 2012) are among the most relevant in the literature regarding this problem. However, these forbidden regions imposed by proxemics for robot navigation are not permanent, as several authors have pointed out, and can vary accordingly to different aspects. Previous experience with the robot (Takayama and Pantofaru, 2009), or the functional noise of the robot (van Berkel, 2013) are examples of aspects that influence on these areas.

Most of social navigation algorithms are based on using a classic navigation algorithm, and therefore adding social conventions and/or social constraints. According to this paradigm, some authors have proposed models of social rules by using cost functions. In (Kirby, 2010), for instance, the authors use a classical A* path planner in conjunction with social conventions, such as to pass humans on the right. In the Traberg et al.'s work Hansen et al. (2009), they use potential fields and a proxemics model. Works like (Luber et al., 2012) demonstrates that navigation algorithms based on proxemic are not always the best choice, and there exist more attributes that provide in robot socially agreeable cruising. There exist other solutions for social navigation which use the detection of human intentions in order to model the social navigation. In (Ratsamee et al., 2013), authors propose the Modified Social Force Model (MSFM), basically a local navigation method where the path is able to be modified after analyzing the human intention. Other Social Force Model where used in (Ferrer et al., 2013) for robot interaction. Also, different works study learning navigation behaviors through different methods, such as inverse reinforcement learning (Henry et al., 2010; Kretzschmar et al., 2016; Okal and Arras, 2016b), RTT planner (Pérez-Higueras et al., 2016) or maximum entropy learning methods (Kuderer et al., 2012).

When a robot plans the best path in human-populated environments, it must avoid passing between two people talking or getting inside the field of view of the people when they are observing a particular object. Social mapping is an interesting concept recently introduced in the robotics community in order to manage the shared space between humans and robots. In Papadakis et al. (2013) it is proposed a framework that can model context-dependent human spatial interactions, encoded in the form of a social map. The social map is obtained by solving a learning problem using Kernel Principal Component Analysis (KPCA), and later the social borders are calculated as isocontours of the learned implicit function. This work is extended in (Papadakis et al., 2014), where authors suggest a skew-normal probability density in order to model the social space. The authors in (Mead and Matarić, 2016) use a perceptual model that takes into account the relative pose between human and robot, the human gestures and the speech volume for building the social space. Recently, in (Kostavelis et al., 2017) authors present a human-oriented robot navigation strategy where the human space is modeled according to proxemics theory. In summary, the number of works that have incorporated this notion of personal space model in the path planning step has increased in the last years (Charalampous et al., 2017). The work presented in this paper is also based on proxemics theory. Unlike other social navigation algorithms that only use RRT or similar planner, this approach uses a PRM-RRT path planner plus the Elastic Band Path Optimization as the navigation stack. In this paper, personal spaces define forbidden areas for robot navigation. These forbidden regions allow to update the graph of free space and directly re-adapt the path planned by the robot during navigation, which is a significant advantage that similar approaches lack.

Most human-populated scenarios are crowded with people talking in groups at a relatively short distance to each other. In these situations, path planners must take into account groups of

people as *combined entities* instead of multiple single personal spaces. The problem of identifying and correctly representing groups of people in the environment is a challenge itself. Most works dealing with groups of people are built upon the F-formation system (Kendon, 1990; Gómez et al., 2014) or the O-Space (Rios-Martinez, 2013) formalization, which state that people often group themselves in some spatial formation with a shared space between them. In this respect, this paper focuses on an adaptive spatial density function for clustering groups of people in different formations, which defines the shared space according to distances and relative angles between humans. Fig. 2 illustrates the most frequent Kendon's formations or arrangements: N-shape, Vis-a-vis, V-shape, L-shape, C-shape and side-by-side. Besides, the O-space defined in (Rios-Martinez, 2013) is also shown in Fig. 2. All of them have been taken into account in the function described in this paper. The proposed adaptive spatial density function is able to directly –only using this mathematical function– cluster groups of people in different formations, and it defines the shared space according to distances and relative angles between humans.

Regarding interactive scenarios (*i.e.*, spaces in which people and buildings engage in a mutual relationship) some authors define regions next to objects in which robot navigation is forbidden. The space affordances are defined in (Rios-Martinez, 2013) as potential activity spaces, which are social spaces constituted by means of actions performed by humans. A similar idea was previously introduced in (Tipaldi and Arras, 2011a,b), where these areas are considered by means of a spatial Poisson process that allows encoding the probability of human activity events. In (Kostavelis et al., 2017) a concept similar to space affordances is considered by taking into account areas frequently visited in the environment. This paper uses a similar region as the introduced in (Rios-Martinez, 2013) and updates and adapts the robot's navigation plan according to this information. Unlike the proposal in (Rios-Martinez, 2013), this work defines the forbidden region for robot navigation as polylines, which are then used to update the graph of free space and to adapt the path planned by the robot during the navigation.

In summary, the work proposed in this paper defines a mathematical model based on the use of an asymmetric Gaussian function (Kirby, 2010) to model the personal space of an individual. The algorithm proposed also uses a modified version of the density function presented in (Vieira et al., 2014) in order to efficiently analyze the environment and cluster groups of people according to its pattern of arrangement. The concept of space affordances is also included in this paper, where each object in the interactive scenario defines a mathematical model based on a modified version of the algorithm described (Rios-Martinez, 2013). These models are incorporated in the navigation architecture presented in (Haut et al., 2016), allowing the robot to navigate in a more social manner among humans.

3. System overview

In order to plan the best social path in human-populated environments, this paper proposes the following strategy: i) detect and represent humans; ii) determine if the space affordances

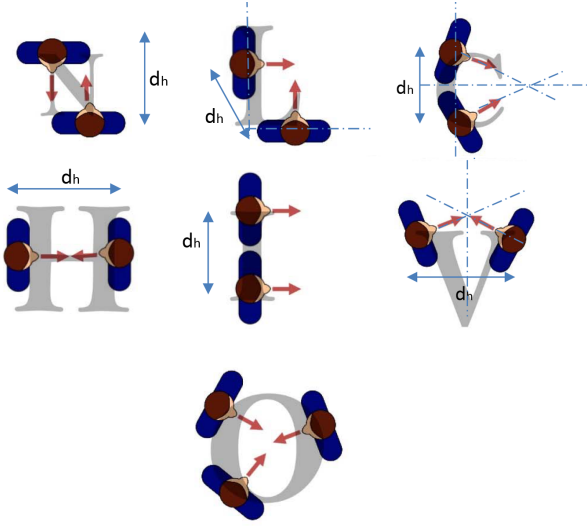


Figure 2: Taxonomies of arrangements for a two-person formation defined in (Kendon, 1990) and three-person formation defined in (Rios-Martinez, 2013). In the figure, d_h is the distance between humans during conversation. The method proposed in this paper adapts the social space according to the arrangement.

are being used as activity spaces to consider them forbidden for navigation; iii) cluster humans into groups according to its social interactions; and iv) include these forbidden spaces in the navigation architecture. The methodology proposed in this paper can be divided into three fundamental steps:

- *Human representation and clustering*: An algorithm which, based on the use of an Asymmetric Gaussian representation for personal space (Kirby, 2010) and the use of a global density function, separates individuals into groups according to its arrangement pattern. Human detection and modelling is assumed to be solved by the CORTEX architecture (Bustos García et al., 2017)
- *Space Affordances*: The space affordances are created by including certain objects with which humans often interact. These areas are defined as trapezoidal spaces which are considered forbidden for navigation when the humans interact with the objects. These space affordances are usually called activity spaces when humans interact with objects (see (Rios-Martinez, 2013)).
- *Socially acceptable navigation*: The social navigation architecture uses the well-known Probabilistic Road Mapping (PRM) (Olson et al., 2006) and Rapidly-exploring Random Tree (RRT) (LaValle, 2006) planners, in conjunction with the *elastic band* algorithm, modified to take into account the social behavior in the path optimization (Haut et al., 2016).

Fig. 3 depicts the proposed approach. In the following sections the social navigation framework is explained in detail.

4. Adaptive Spatial Density Function for Robot Navigation

4.1. Personal space modeling

Considering $S \subset \mathbb{R}^2$ the space of the global map, an individual i is represented by its pose (position and orientation), $\mathbf{h}_i = (x_i \ y_i \ \theta_i)^T$, being $(x_i \ y_i)^T \in S$ and $\theta_i \in [0, 2\pi)$. In order to model the personal space of each individual, an asymmetric 2-dimensional Gaussian function is used (Kirby, 2010). This function associates the distance between a point $\mathbf{p} = (x \ y)^T \in S$ and the person's position with a real value $g_i \in [0, 1]$. The expression for the Gaussian function is

$$g_{h_i}(x, y) = \exp(-(k_1(x - x_i)^2 + k_2(x - x_i)(y - y_i) + k_3(y - y_i)^2)), \quad (1)$$

being k_1 , k_2 and k_3 the coefficients used to take into account the rotation of the function β_i , defined by the relations

$$\begin{aligned} k_1(\beta_i) &= \frac{\cos(\beta_i)^2}{2\sigma^2} + \frac{\sin(\beta_i)^2}{2\sigma_s^2} \\ k_2(\beta_i) &= \frac{\sin(2\beta_i)}{4\sigma^2} - \frac{\sin(2\beta_i)}{4\sigma_s^2} \\ k_3(\beta_i) &= \frac{\sin(\beta_i)^2}{2\sigma^2} + \frac{\cos(\beta_i)^2}{2\sigma_s^2} \end{aligned}$$

where σ_s is the variance to the sides ($\beta_i \pm \pi/2$ direction) and represents the variance along the β_i direction (σ_h) or the variance to the rear (σ_r) (see (Kirby, 2010)). In Fig. 4 an example of the personal space model is shown.

Once calculated the personal space for each individual in the environment, it is used as the input of a global density function that clusters the humans, as the next section explains.

4.2. People clustering

According to (Kendon, 1990), for two people in conversation, six arrangements are the most frequent depending of the kind of scenario, *e.g.*, spaces open, spaces that are semi-open and spaces where there is no pedestrian movement. These typical formations are shown in Fig. 2. In interactions of more than two people, typical formations are defined as O-spaces (Rios-Martinez, 2013). Therefore, it is needed to define how to associate the various personal spaces of each individual when considering groups of humans. This association is accomplished by performing a Gaussian Mixture.

Let $g_{h_i}(\mathbf{p})$ be the personal space function for each individual i in the set of all P of all people in S . The global density space function $G_d(\mathbf{p})$ is defined as:

$$G_d(x, y) = \sum_{i \in P} g_{h_i}(x, y). \quad (2)$$

Once performed the association and calculated the value of $G_d(\mathbf{p})$, the next stage is to separate people in groups. The method described in this paper defines regions of forbidden navigation by discriminating the group contour to which each human belongs. This is done using a modified version of the method described in Vieira's work (Vieira et al., 2014), which is employed for grouping points in point clouds, clustering them in different objects.

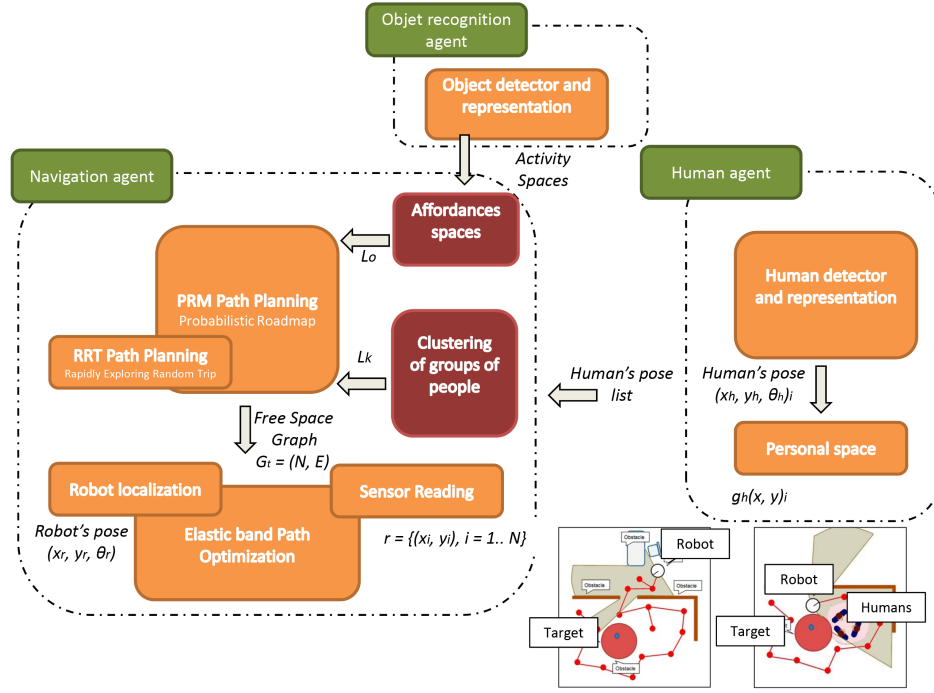


Figure 3: Overview of the social navigation framework presented in this paper.

In order to group individuals into clusters, the method chooses the Ω_d and Ω_θ parameters as the *smallest Euclidean distance and the smallest difference of angles between two people* $\mathbf{h}_i(\mathbf{x}, \mathbf{y}, \theta)$, $\mathbf{h}_j(\mathbf{x}, \mathbf{y}, \theta) \in P$ such that those two are neighbours. These values are given by the insights of proxemics. If $\mathbf{h}_i(\mathbf{x}, \mathbf{y})$ and $\mathbf{h}_j(\mathbf{x}, \mathbf{y})$ are neighbours, then $\|\mathbf{h}_i(\mathbf{x}, \mathbf{y}), \mathbf{h}_j(\mathbf{x}, \mathbf{y})\| \leq \Omega_d$ and $\|\mathbf{h}_i(\theta), \mathbf{h}_j(\theta)\| \leq \Omega_\theta$, and the density contribution δ between them is

$$\delta = g_{h_i}(\mathbf{h}_j). \quad (3)$$

Since $g_{h_i}(\mathbf{h}_i) = 1$ for each $\mathbf{h}_i \in P$, then if \mathbf{h}_i has k neighbours then $G(\mathbf{h}_i) \geq 1 + k\delta$. Hence, the method can adjust a density threshold ϕ in order to group individuals who have at least k neighbours. ϕ is given by

$$\phi = 1 + k\delta, \quad (4)$$

and it can compare the value of the global function for each point in S and determine whether that point belongs to the personal space of a group of individuals. The set of such points is denoted by J and given by the expression

$$J = \{\mathbf{h} \in S \mid G_d(\mathbf{p}) \geq \phi\}. \quad (5)$$

It can be controlled how near or far the border of J is in relation to each human in the cluster by manipulating the value of ϕ either by setting it directly or by manipulating the value of δ . In the next section a validation of this parameter ϕ is described. Fig. 5b shows the result of applying this procedure to the group shown in Fig. 5a.

Finally, the contours of these forbidden areas are defined by a set of k polygonal chain (*i.e.*, polyline) $L_k = \{l_1, \dots, l_k\}$, where k is the number of regions detected by the algorithm. The

use of this polygonal chain L_k allows to work in a continuous world representation. The curve l_i is described as $l_i = \{a_1, \dots, a_m\}$, being $a_i = (x, y)$; the vertices of the curve, which are located in the contour of the region J . The number of vertices, m , is dynamically adjusted by the algorithm, being the Euclidean distance between two consecutive vertices, $d(a_i, a_j)$, less than a fixed threshold d_l .

5. Space Affordances

Let $O_n = \{o_1, \dots, o_n\}$ be the set of objects with which humans usually interact in the environment, where n is the number of objects detected by the agent. It is assumed that these objects are detected by the robot's perception system (Bustos García et al., 2017). Each object o_i stores the interaction space i_{o_i} as an attribute, which is associated to the space required to interact with this object, and also its pose in S , $p_{o_i} = (x, y, \theta_i)$,

$$o_i = (p_{o_i}, i_{o_i})$$

Different objects in the environments have different interaction spaces, for instance, to use a coffee machine it is needed less space than the needed to read a poster, because it can be done from a farther distance. Next, the space affordance A_{o_i} is defined for each object $i \in O$. In this paper, the shape of these spaces has been modeled as a symmetrical trapezoid with height a_h and widths (a_{w1}, a_{w2}) , as is shown in Fig. 6, being $a_{w2} = \frac{a_{w1} \cdot a_h}{4}$.

Once the space affordance A_{o_i} is created, it is checked if is being used as an activity space, what means that the person is interacting with the object. Two conditions have to be fulfilled to consider that an activity is being carried out: i) the person has to be inside the space affordance, *i.e.*, $h_i \in A_{o_i}$; and ii) h_j has

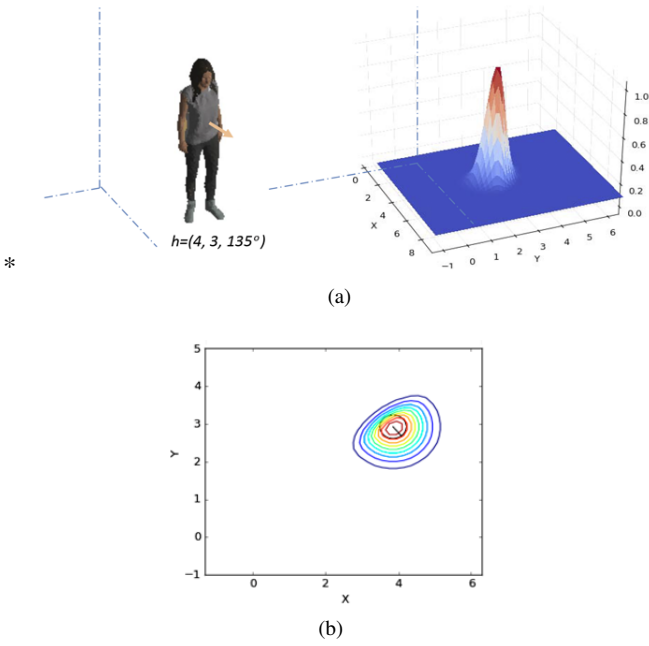


Figure 4: (a) Personal space of a single individual is modeled by Equation (1); (b) the person is posed at $\mathbf{h} = [4.0m \ 3.0m \ 135^\circ]^T$.

to be looking at the object o_i . The space will be forbidden for navigation *iff* these conditions are true. Similar to the personal space described in Section 4, A_{o_i} is also modeled by a polyline that is described by four vertices v_a that will be used to delimit forbidden areas for navigation. Finally, $L_o = \{A_{o_1}, \dots, A_{o_n}\}$ describes the set of polylines used by the navigation algorithm for defining forbidden navigation areas.

In Fig. 7a four humans in different positions and four objects are shown (a coffee machine, a fridge, a phone, and a pin board). Some of the humans are interacting with the objects. The position of the humans, the objects and the shapes of the spaces created for these objects are shown in Fig. 7. The vertices v_a are shown in green if the space is being considered as free. These vertices are in green even if the person is inside the space but is not looking at the object. A red vertex means that the person is inside the space affordance and looking at the object, so the space is being used as an activity space and therefore considered as occupied.

6. Social navigation in human-populated environment

6.1. Socially Acceptable Navigation

Once the polygonal curves associated to each group of humans, L_k , and the space affordances, S_a , have been calculated, the proposed approach integrates this information in the path planner. First, the global planner traces a navigation plan for a given target $\mathbf{T} \in S$. Then, the local planner modifies the plan according to the obstacles and humans detected by the robot's sensor. In the proposed approach, the social navigation architecture is a modified version of the one presented in (Haut et al., 2016), which consists of the next stages:

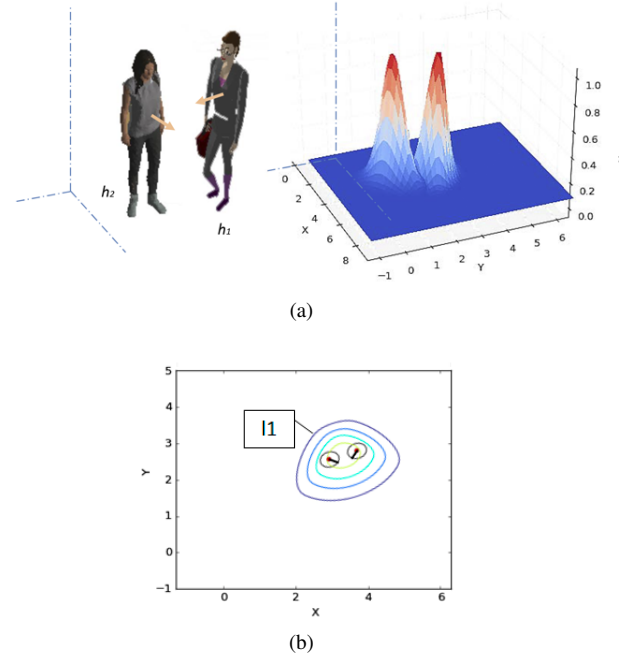


Figure 5: (a) shows a group of two people in points $\mathbf{q}_1 = [3m, 4m]^T$ and $\mathbf{q}_2 = [3m, 1.28m]^T$, with orientations $\theta_1 = 135^\circ$ and $\theta_2 = 335^\circ$ respectively. Both two gaussians are also drawn. (b) shows the result of applying the clustering algorithm to these groups with $\phi = 1.0$.

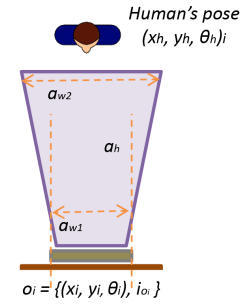


Figure 6: Space affordance of an interactive object is modeled by a symmetrical trapezoid.

1. *PRM-RRT path planners.* First, a graph of the free space is created using a generalized inverse kinematics algorithm, based on the Levenberg-Marquardt method. This graph is used by the PRM planner (Olson et al., 2006) to search for a path free of obstacles from the robot location to the target. In case that the graph still had more than one connected region or there was not a direct line of sight from the robot (or the target) to the graph, the RRT planner (LaValle, 2006) is used. Thus, the final graph that describes the free space is defined by a set of nodes, N , and edges, E , $G_t = (N, E)$. In Fig. 8, a descriptive example of this graph is drawn as a set of nodes (red circles) and arcs (red lines). Next, the path is created by first searching the closest point in the graph to the current robot's pose, the closest point in G_t to the target position T and a path through the graph linking both points.
2. *Elastic Band Path Optimization* For the path optimization, the initial path is transformed into a evenly separated series

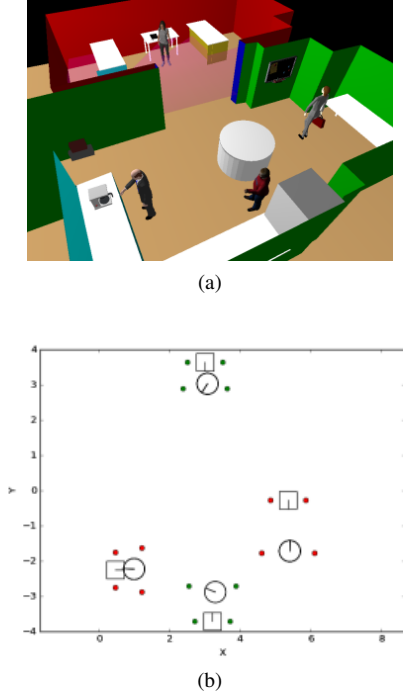


Figure 7: Four objects (a coffee machine, a fridge, a phone, and a pin board) and four humans in different poses are included in the interactive scenario. activity spaces are illustrated in the figure.

of way-points, at a distance closer than the length of the robot. The elastic band path optimization (Haut et al., 2016) updates the path planned for each step as it is traversed, adapting it to unexpected events, such as obstacles or group of humans described by the list of polylines L_k . As illustrated in Fig. 8, the path is analyzed under the laser range, and two virtual forces are created. Let's define the path $P = p_i \in \mathbb{R}^2$ as an ordered set of $(x, y) \in S$ points – called steps – of the robot's configuration space. Then, an internal contraction virtual force is defined to model the tension in a physical elastic band using the following equation:

$$f_c = k_c \cdot \left(\frac{p_{i-1} - p_i}{\|p_{i-1} - p_i\|} + \frac{p_{i+1} - p_i}{\|p_{i+1} - p_i\|} \right), \quad (6)$$

where p_i is the position of step i in the path. The physical interpretation is a series of springs connecting the path steps, with k_c as a global contraction gain. These contraction forces are illustrated in green color in Fig. 8.

Also, a repulsive force is created to push each step away from the obstacles and humans defined by L_k to increase the clearance of the robot. A function $d(p)$ is defined $\mathbb{R}^2 \times \mathbb{R}^2 \rightarrow \{R^+ \cup 0\}$ that computes the minimum distance of a step p to the nearest obstacle, as perceived by the laser sensor.

$$f_r = \begin{cases} k_r(\rho_0 - \rho(p)) \frac{\partial \rho}{\partial p} & p < \rho_0 \\ 0 & p \geq \rho_0 \end{cases}, \quad (7)$$

where k_r is a global repulsion gain and represents the maximum distance up to which the force is applied. These repulsion forces are illustrated in blue color in Fig. 8. The Jacobian $\frac{\partial \rho}{\partial p}$ is approximated using finite differences. The

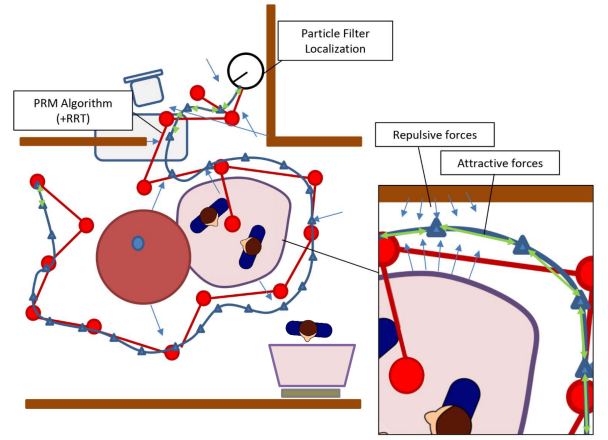


Figure 8: The final social path is shown as the blue continuous line (Δ). Besides, the graph G_r provided by path planners (red color), and the set of forces are drawn.

final force is calculated as a linear combination of both, $f = f_c + f_r$, that is continuously applied to each step inside the laser field. This force modifies the final path, as shown in Fig. 8.

7. Experimental results

7.1. Adaptive spatial density function assessment

The proposed system has two parameters that can be tuned to properly adjust the robot navigation behavior to the social context:

- d_l : the maximum Euclidean distance between consecutive vertices in the polyline. A specific value is proposed.
- ϕ : the density threshold. The value proposed depends how the humans are interacting (see the formations proposed in (Kendon, 1990)).

The distance threshold parameter d_l allows to adjust the density of vertices in the polyline. The smaller the value of d_l the higher the detail of the shape of the forbidden area. In order to choose an appropriate d_l value, several simulated experiments with different individuals were conducted. The tests showed that, below 10cm approximately, decreasing the value of the parameter did not considerably affect the shape of the resulting forbidden area. The conclusion drawn from the experiments is that d_l can be safely fixed to 10cm.

The parameter ϕ allows to correctly cluster individuals according to their formation during a conversation, and to adapt how much the robot can approach to people. To estimate a proper value for ϕ for the used experimental set-up, a set of simulated experiments were conducted. These experiments involved humans in different formations and distances between them (d_h). Table 1 shows the output of the clustering algorithm for different values of ϕ and the distance between humans in the different formations (*i.e.*, N-shape, Vis-a-vis, V-shape, L-shape, C-shape and Side-by-side). The selected ϕ value is adapted according to the formation (red color in Table 1).

Table 1: Different two-person formations and results of the clustering algorithm in function of the threshold ϕ and the distance between humans d_i .

N-shape			Vis-a-Vis		
ϕ	Distance	Cluster (Y/N)	ϕ	Distance	Cluster (Y/N)
0.1	50 cm	Y	0.1	50 cm	Y
	100 cm	Y		100 cm	Y
	150 cm	Y		150 cm	Y
	200 cm	Y		200 cm	Y
0.3	50 cm	Y	0.3	50 cm	Y
	100 cm	Y		100 cm	Y
	150 cm	Y		150 cm	Y
	200 cm	N		200 cm	N
0.5	50 cm	Y	0.5	50 cm	Y
	100 cm	Y		100 cm	Y
	150 cm	N		150 cm	Y
	200 cm	N		200 cm	N
0.7	50 cm	Y	0.7	50 cm	Y
	100 cm	Y		100 cm	Y
	150 cm	N		150 cm	N
	200 cm	N		200 cm	N
0.9	50 cm	Y	0.9	50 cm	Y
	100 cm	N		100 cm	Y
	150 cm	N		150 cm	N
	200 cm	N		200 cm	N

V-shape			L-shape		
ϕ	Distance	Cluster (Y/N)	ϕ	Distance	Cluster (Y/N)
0.1	50 cm	Y	0.1	50 cm	Y
	100 cm	Y		100 cm	Y
	150 cm	Y		150 cm	Y
	200 cm	Y		200 cm	Y
0.3	50 cm	Y	0.3	50 cm	Y
	100 cm	Y		100 cm	Y
	150 cm	Y		150 cm	Y
	200 cm	N		200 cm	N
0.5	50 cm	Y	0.5	50 cm	Y
	100 cm	Y		100 cm	Y
	150 cm	N		150 cm	Y
	200 cm	N		200 cm	N
0.7	50 cm	Y	0.7	50 cm	Y
	100 cm	Y		100 cm	Y
	150 cm	N		150 cm	N
	200 cm	N		200 cm	N
0.9	50 cm	Y	0.9	50 cm	Y
	100 cm	N		100 cm	Y
	150 cm	N		150 cm	N
	200 cm	N		200 cm	N

C-shape			Side-by-side		
ϕ	Distance	Cluster (Y/N)	ϕ	Distance	Cluster (Y/N)
0.1	50 cm	Y	0.1	50 cm	Y
	100 cm	Y		100 cm	Y
	150 cm	Y		150 cm	Y
	200 cm	Y		200 cm	Y
0.3	50 cm	Y	0.3	50 cm	Y
	100 cm	Y		100 cm	Y
	150 cm	Y		150 cm	Y
	200 cm	N		200 cm	N
0.5	50 cm	Y	0.5	50 cm	Y
	100 cm	Y		100 cm	Y
	150 cm	Y		150 cm	Y
	200 cm	N		200 cm	N
0.7	50 cm	Y	0.7	50 cm	Y
	100 cm	Y		100 cm	Y
	150 cm	N		150 cm	N
	200 cm	N		200 cm	N
0.9	50 cm	Y	0.9	50 cm	Y
	100 cm	Y		100 cm	Y
	150 cm	N		150 cm	N
	200 cm	N		200 cm	N

7.2. Navigation in real and Simulated scenarios

Real and simulated scenarios were used to validate the performance of the proposed algorithm. The algorithms have been developed in several C++ components using the RoboComp framework¹. The tests in simulated scenarios were performed on a computer with an Intel Core i5 2.4GHz processor with 4Gb of DDR3 RAM and Ubuntu GNU/Linux 16.10. The robot used in the real tests is Shelly, an omnidirectional autonomous manipulator (see Fig. 10.b). Shelly uses the robotics cognitive architecture CORTEX (Bustos García et al., 2017), which was designed to create flexible behaviours in social robots. CORTEX is organized as a set of cooperating agents that communicate through a shared representation (i.e., *Deep State Representation*). Fig. 9 shows an overview of CORTEX and its main software agents. Human recognition agent detects and tracks human's

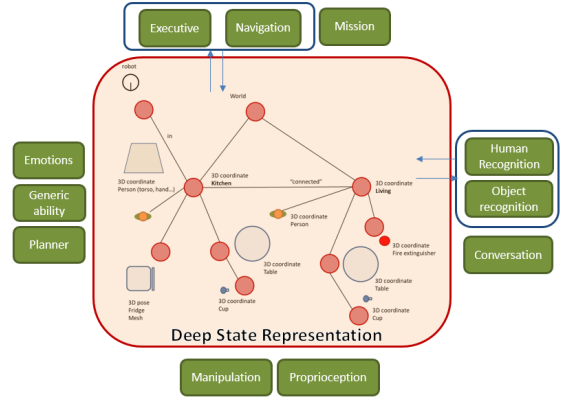


Figure 9: Main agents within CORTEX involved in the social navigation system described in this proposal are highlighted in red

pose (position and orientation), and also updates these values on the shared representation.

In order to assess the effectiveness of the proposed navigation approach, the methodology has been evaluated accordingly to these metrics in both static scenarios: (i) average minimum distance to a human during navigation, d_{min} ; (ii) distance travelled, d_t ; (iii) navigation time, τ ; (iv) cumulative heading changes, CHC ; and (v) personal space intrusions, Psi . These metrics have been already established by the scientific community (see (Kostavelis et al., 2017; Okal and Arras, 2016a,b)) and thus the proposed methodology follows a scheme that is similar to the one followed by other developments and works in the literature. A brief description of these metrics are described as follows:

- Average distance to the closest human during navigation: A measure of the average distance from the robot pose, $x_r(x, y, \theta)$, to the closest human $h_i(x, y, \theta)$ along the robot's path $P = \{x_r^j(x, y, \theta) \mid j = 1, 2, \dots, N\}$, being N the number of points of the trajectory.

$$d_{min} = \min_i \{ \|x_r^j(x, y) - h_i(x, y)\| \} \quad (8)$$

- Distance travelled: length of the robot's path, in meters.

$$d_t = \sum_{j=1}^{j=N-1} \|x_r^j(x, y) - x_r^{j+1}(x, y)\| \quad (9)$$

- Navigation time: time since the robot starts the navigation, τ_{ini} , until it arrives to the target, τ_{end} .

$$\tau = \tau_{end} - \tau_{ini} \quad (10)$$

- Cumulative heading changes: a measure to count the cumulative heading changes of the robot during navigation (Okal and Arras, 2016b). Angles are then normalized between $-\pi$ and π .

$$CHC = \frac{1}{N} \sum_{j=1}^{j=N-1} \|x_r^j(\theta) - x_r^{j+1}(\theta)\| \quad (11)$$

¹<https://github.com/robocomp>

- Personal space intrusions (Psi): In this paper, four different areas are defined: Intimate ($\|x_r^j(x, y) - h_i(x, y)\| \leq 0.45m$); Personal ($0.45m \leq \|x_r^j(x, y) - h_i(x, y)\| \leq 1.2m$); Social ($1.2m \leq \|x_r^j(x, y) - h_i(x, y)\| \leq 3.6m$); and Public ($\|x_r^j(x, y) - h_i(x, y)\| \geq 3.6m$). Along the robot's path, this metric measures the percentage of the time spent in each area as:

$$Psi = \left\{ \frac{1}{N} \sum_{i=1}^{i=N} \mathcal{F} \|x_r^j(x, y) - h_i(x, y)\| \leq \delta^k \right\} \quad (12)$$

where δ^k defines the distance range for classification (intimate, personal, social and public), and $\mathcal{F}()$ is the indicator function.

A comparative study of the proposal with the no human aware navigation architecture presented in (Haut et al., 2016) is also provided. The principal difference between these two navigation architectures is the social behavior defined in this paper, which allows to conclude if there is significant improvements in navigation results. Besides, this set of metrics facilitates to compare the social navigation results with other similar approaches.

The real scenario is a $65m^2$ three-room apartment equipped with a kitchen, a bathroom and a living room. In this apartment, the same two people talk in a vis-a-vis formation in different poses, being $d_h = 1.2m$. The robot Shelly navigates through this apartment to several positions². Fig. 10 shows the setup of the experiment. The individuals are grouped as shown in Fig. 10a. Initial robot's pose and the different intermediate targets are also presented in Fig. 10b. A frame of the video recorded during the tests is shown in Fig. 10c. Fig. 11 describes the different stages of the mechanism proposed in this paper to detect and determine the size and shape of forbidden areas. In Fig. 11a, the discomfort experienced by the individuals is modeled using different curve lines of each Gaussian function. Fig. 11b shows the resulting global discomfort function. Fig. 11c and Fig. 11d show the polylines of the groups of people after clustering, in a plot and in the internal geometric model of the robot, respectively. These clusters describe the forbidden areas for the robot navigation and are related with the ϕ parameter ($\phi = 0.7$).

The simulated scenario is a recreation of the same real apartment with 6 individuals in different formations (see Fig. 12a), where the robot navigates between different targets. The original graph of free space is shown in Fig. 12b. The isocontour lines of the discomfort function used to compute the personal space are shown in Fig. 12c. Fig. 12d depicts the clusters of people after using the algorithm.

Finally, a comparative study of the proposed navigation methodology and the navigation system without social awareness (Haut et al., 2016) is included. For the real experiment, the robot had to perform two different navigation missions, manoeuvring in a socially acceptable way. A set of intermediate targets was defined in order to force robot to disturb people (marked in Fig. 10b). Each path has been repeated 10 times. The mean values of the time used by the robot during its navigation, τ , so as its travelled distance, d_t , are shown in Table 2. The mean

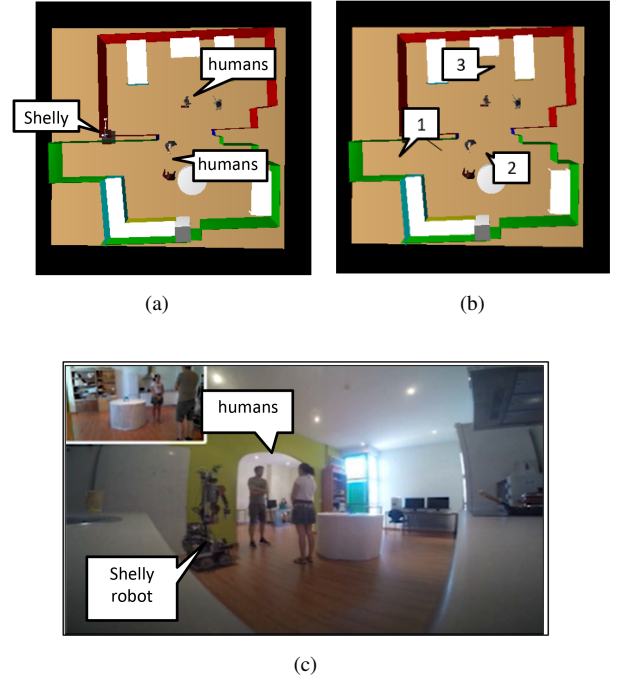


Figure 10: a) A representation of the real apartment used in the tests. The robot Shelly must socially navigate between two groups of people in a vis-a-vis formation. b) initial robot's position (labeled as 1) and intermediate robot's target (labeled as 2 and 3). c) A frame of the video recorded during the real tests.

values of the minimum distances to each individuals, d_{min} , the cumulative heading changes, CHC , and the Personal space intrusions (Psi) for each area are also shown in Table 2. The same information for simulated environment is summarized in Fig. 3. The tests were achieved 10 times in the simulated environment using always the same targets and positioning of objects and people. In particular, d_{min} values using the navigation architecture proposed in this work are higher than the navigation method without social skills. These d_{min} values allow the robot to move around humans without disturbing them. The total time (τ) to reach the targets is higher, but it is normal due to the greater distance travelled (d_t). An interesting result is given by Psi values: in the proposed approach the robot never navigates in the intimate area, $Psi(Intimate)$, but this value is different to zero if the robot navigates using the approach described in (Haut et al., 2016). Other metric, such as CHC , has similar values, and it provides information about the smoothness of the path, which is acceptable compared to other approaches in the literature.

From the results of the experiments, it is possible to conclude that the robot presents notable advantages in social navigation behavior, avoiding groups of individuals. The metrics used in this paper facilitates the comparison of the proposed approach with other similar state-of-art works. However, as other authors indicate (Sutcliffe et al., 2015), without a user study it is difficult to assess if the proposed navigation system is more comfortable for the humans nearby. Table 4 summarizes the main social behaviors during navigation- typically accepted by physiologists and sociologists –that are achieved by using the approach described in this paper.

²A video of the real tests is accessible on <https://youtu.be/2jRp18AUuLU>

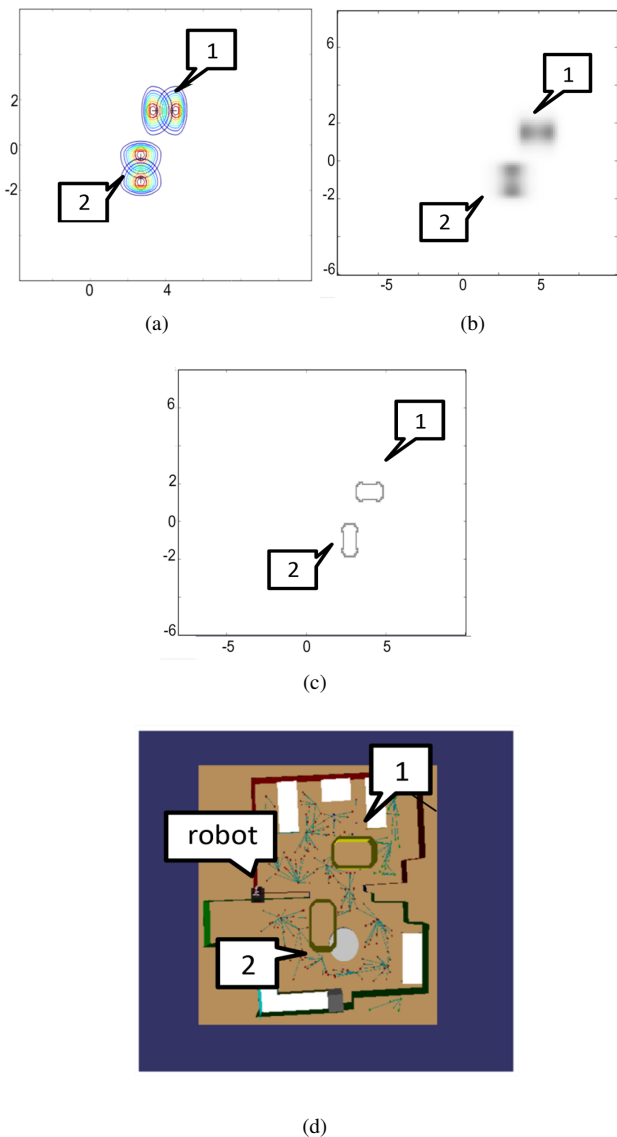


Figure 11: a) Four people are located in the real apartment in a vis-a-vis formation; b) discomfort function; c) polylines generated by the algorithm; and d) Polylines are used in the path-planning algorithm to modify the graph of free space.

7.3. Navigation in interactive scenarios with space affordances

To test the algorithm created to consider the space affordances, a rectangular simulated environment with a whiteboard on it has been used. The simulated environment is shown in Fig. 13a. The object has been placed in the position $x = 2m$, $y = 4.5m$ with $a_s = 3m$ in order to create a space affordance which the robot has to avoid if people in the environment are interacting with it, what means that the space affordance is being used as an Activity Space. The resulting space affordance is shown in Fig. 13b.

A single human, placed in front of the object in the position $x = 2m$, $y = 2m$, has been used for this test. The robot has had to navigate from the position $x = -0.8m$, $y = 3m$ to $x = 4.5m$, $y = 3m$, avoiding the space affordance of the object if the person is interacting with it.

Table 2: Navigation results for the real apartment. For each variable it is provided the mean and the standard deviation in parenthesis.

Parameter	Social navigation architecture	(Haut et al., 2016)
d_t (m)	8.03 (0.12)	6.0 (0.14)
τ (s)	52 (0.94)	50 (1.41)
CHC	3.33 (0.09)	3.107 (0.26)
d_{min} Person 1 (cm)	188 (0.07)	26 (0.05)
d_{min} Person 2 (cm)	79 (0.05)	61 (0.3)
Ψ (Intimate) (%)	0 (0)	11.13 (0.29)
Ψ (Personal) (%)	25.0 (4.6)	27.95 (1.66)
Ψ (Social + Public) (%)	74.9 (4.6)	60.91 (1.95)
d_t (m)	8.64 (0.45)	6.49 (0.075)
τ (s)	59 (7.4)	52 (0.47)
CHC	4.2 ()	3.54 (0.26)
d_{min} Person 1 (m)	167 (0.077)	88 (0.8)
d_{min} Person 2 (m)	83 (0.067)	32 (0.033)
Ψ (Intimate) (%)	0 (0)	9.9 (1.98)
Ψ (Personal) (%)	43.04 (0.87)	38.76 (5.57)
Ψ (Social + Public) (%)	56.95 (0.87)	51.30 (4.21)

Table 3: Navigation results for the simulated apartment. For each variable it is provided the mean and the standard deviation in parenthesis.

Parameter	Social navigation architecture	(Haut et al., 2016)
d_t (m)	21.99 ()	20.12
τ (s)	175	140
CHC	5.26	3.54
d_{min} Person 1 (m)	1.7 (0.01)	0.45 (0.01)
d_{min} Person 2 (m)	1.08 (0.01)	0.52 (0.0)
d_{min} Person 3 (m)	0.79 (0.01)	0.43 (0.01)
d_{min} Person 4 (m)	1.37 (0.02)	0.75 (0.01)
d_{min} Person 5 (m)	0.96 (0.01)	0.71 (0.0)
d_{min} Person 6 (m)	1.14 (0.0)	0.58 (0.01)
Ψ (Intimate) (%)	0 (0)	5.07 (0.22)
Ψ (Personal) (%)	42.62 (3.39)	58.83 (0.41)
Ψ (Social + Public) (%)	57.37 (3.39)	36.09 (0.35)

The same test has been carried out with and without space affordances. The comparison between the different paths the robot took can be seen in Fig. 13c, where it is marked in red the path without space affordances and in blue the path considering them. It can be noticed that, in the first case, the robot has interrupted the human in the performance of its activity.

Table 5 shows the results of navigation with and without space affordances, and it summarizes the time the robot needed to reach the target and the total distance travelled. It also indicates whether the activity performed by the human has been interrupted or not.

8. Conclusion and Future Works

The increasing use of mobile robots in social contexts increases the importance of providing them with the ability to behave in the most socially acceptable way possible. A major issue concerning human-aware path planning problems is related to the people's level of discomfort, which can be represented by proxemic zones.

This work proposed the use of an adaptive spatial density function for social navigation in static environments with humans. This density function is used to efficiently cluster individuals into groups according to their spatial arrangement. This paper

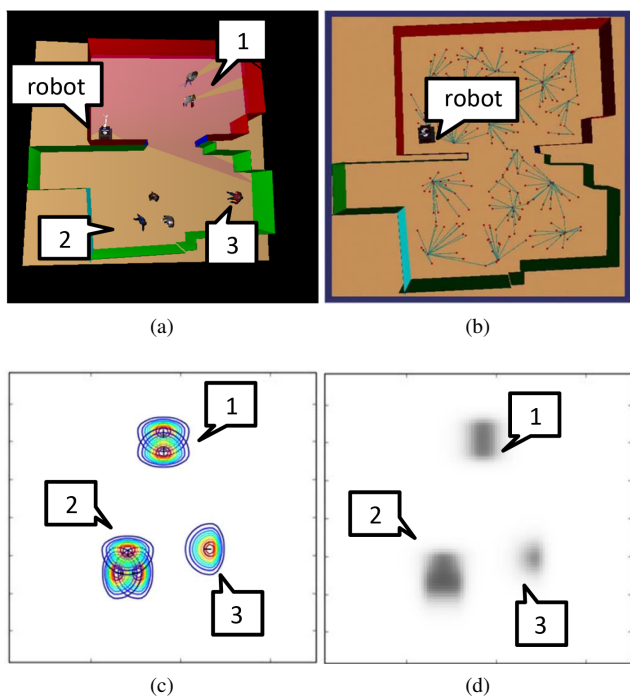


Figure 12: a) 3D visualization of the simulated environment; b) Initial graph generated for the path planners; c) Potential regions of discomfort of the humans is modeled using Mixture of Gaussians; and d) cluster of people, which define the forbidden regions for navigation.

Table 4: Qualitative results of the proposed social navigation system

Social behaviors	Is it achieved?
Human and obstacle avoidance behavior	✓
Social spatial behaviour	✓
Social path-planning behavior	✓

also presented a mathematical model for defining the space affordances associated to each object in the scene. The navigation architecture is modified to execute the navigation considering this social representation. The performance of the approach and the improvement of the robot's social behavior during its motion in human-populated environments are demonstrated in the experiments.

As future research directions we intend to consider others aspects besides navigation, for example, approaching groups of people and initiating an interaction. Future improvements of the system must consider dynamic scenarios where people are not static and their poses are changing. The use of multi-robot systems will also be the focus of future studies.

Acknowledgments

This work has been partially supported by the MICINN Project TIN2015-65686-C5-5-R, by the Extremaduran Government project GR15120, by the Red de Excelencia "Red de Agentes Físicos" TIN2015-71693-REDT, FEDER project 0043-EUROAGE-4-E (Interreg V-A Portugal-Spain (POCTEP) Program), MEC project PHBP14/00083 and by CAPES-DGPU 7523/14-9.

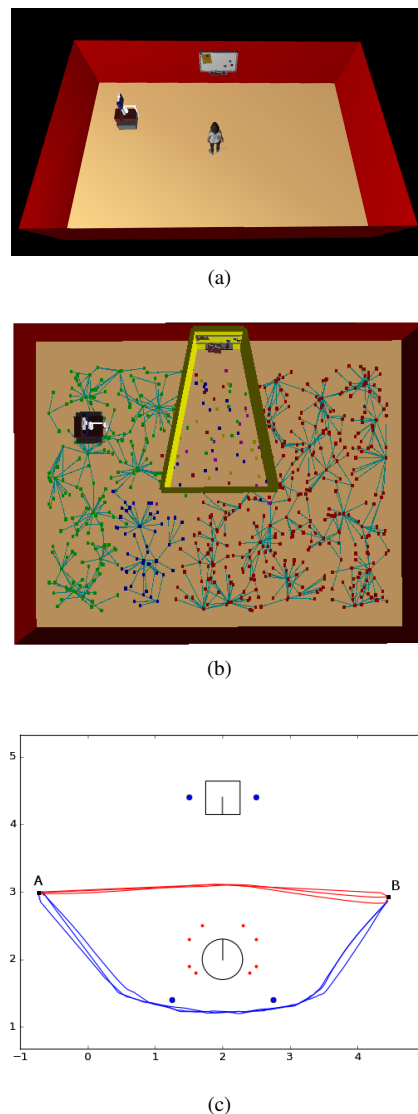


Figure 13: An interactive scenario for the tests described in Section 7.3: a) setup of the experiment; b) activity space for the panel; and c) in blue color: paths followed by the robot using the system proposed in this paper. In red color: paths followed by the robot using the classical navigation algorithm.

References

- van Berkel, N., 2013. How adjustments to the velocity and functional noise of a robot can enhance the approach experience, in: Proc. of TSConIT.
- Bustos García, P., Manso, L.J., Bachiller Burgos, P., Núñez Trujillo, P., 2017. Navigation among people with cortex, in: REACTS workshop at the International Conference on Computer Analysis and Patterns, CAIP, Ystad Saltsjöbad.
- Charalampous, K., Kostavelis, I., Gasteratos, A., 2016. Robot navigation in large-scale social maps: An action recognition approach. *Expert Systems with Applications* 66, 261–273.
- Charalampous, K., Kostavelis, I., Gasteratos, A., 2017. Recent trends in social aware robot navigation: A survey. *Robotics and Autonomous Systems* 93, 85–104.
- Ferrer, G., Garrell, A., Sanfeliu, A., 2013. Robot companion: A social-force based approach with human awareness-navigation in crowded environments, in: Intelligent robots and systems (IROS), 2013 IEEE/RSJ international conference on, IEEE. pp. 1688–1694.
- Gómez, J.V., Mavridis, N., Garrido, S., 2014. Fast marching solution for the social path planning problem, in: Robotics and Automation (ICRA), 2014 IEEE International Conference on, IEEE. pp. 2243–2248.

Table 5: Navigation results with space affordances

Navigation with space affordances		Navigation without space affordances	
Parameter	Value	Parameter	Value
d_t	6.76m	d_t	5.18m
τ	54s	τ	31s
Interruption (Y/N)	N	Interruption (Y/N)	Y

- Hall, E.T., 1966. *The Hidden Dimension: Man's Use of Space in Public and Private*. The Bodley Head Ltd.
- Hansen, S., Svenstrup, M., Jorgen, H., Bak, T., 2009. Adaptive human aware navigation based on motion pattern analysis, in: *Robot and Human Interactive Communication, 2009. RO-MAN 2009. The 18th IEEE International Symposium on*, IEEE. pp. 927–932.
- Haut, M., Manso, L., Gallego, D., Paoletti, M., Bustos, P., Bandera, A., Romero-Garcés, A., 2016. A navigation agent for mobile manipulators, in: *Robot 2015: Second Iberian Robotics Conference*, Springer. pp. 745–756.
- Henry, P., Vollmer, C., Ferris, B., Fox, D., 2010. Learning to navigate through crowded environments, in: *Robotics and Automation (ICRA), 2010 IEEE International Conference on*, IEEE. pp. 981–986.
- Kendon, A., 1990. *Conducting interaction: Patterns of behavior in focused encounters*. volume 7. CUP Archive.
- Kessler, J., Schroeter, C., Gross, H.M., 2011. Approaching a person in a socially acceptable manner using a fast marching planner, in: *International Conference on Intelligent Robotics and Applications*, Springer. pp. 368–377.
- Kirby, R., 2010. *Social robot navigation*. Carnegie Mellon University.
- Kostavelis, I., 2017. Robot Behavioral Mapping: A Representation that Consolidates the Human-robot Coexistence. *Robotics and Automation Engineering* 1, 1–3.
- Kostavelis, I., Kargakos, A., Giakoumis, D., Tzovaras, D., 2017. Robot's workspace enhancement with dynamic human presence for socially-aware navigation, in: *International Conference on Computer Vision Systems*, Springer. pp. 279–288.
- Kretzschmar, H., Spies, M., Sprunk, C., Burgard, W., 2016. Socially compliant mobile robot navigation via inverse reinforcement learning. *The International Journal of Robotics Research* 35, 1289–1307.
- Kruse, T., Basili, P., Glasauer, S., Kirsch, A., 2012. Legible robot navigation in the proximity of moving humans, in: *Advanced Robotics and its Social Impacts (ARSO), 2012 IEEE Workshop on*, IEEE. pp. 83–88.
- Kruse, T., Pandey, A.K., Alami, R., Kirsch, A., 2013. Human-aware robot navigation: A survey. *Robotics and Autonomous Systems* 61, 1726–1743.
- Kuderer, M., Kretzschmar, H., Sprunk, C., Burgard, W., 2012. Feature-based prediction of trajectories for socially compliant navigation., in: *Robotics: science and systems*, Citeseer.
- LaValle, S.M., 2006. *Planning algorithms*. Cambridge university press.
- Luber, M., Spinello, L., Silva, J., Arras, K.O., 2012. Socially-aware robot navigation: A learning approach, in: *Intelligent robots and systems (IROS), 2012 IEEE/RSJ international conference on*, IEEE. pp. 902–907.
- Mead, R., Matarić, M.J., 2016. Perceptual models of human-robot proxemics, in: *Experimental Robotics*, Springer. pp. 261–276.
- Mead, R., Matarić, M.J., 2012. A probabilistic framework for autonomous proxemic control in situated and mobile human-robot interaction, in: *Proc. of 7th ACM/IEEE International Conference on Human-Robot Interaction (HRI)*, pp. 193–194. doi:10.1145/2157689.2157751.
- Mumm, J., Mutlu, B., 2011. Human-robot proxemics: physical and psychological distancing in human-robot interaction , 331–338.
- Núñez, P., Manso, L.J., Bustos, P., Drews-Jr, P., Macharet, D.G., 2016. A proposal for the design of a semantic social path planner using cortex, in: *Workshops on Physical Agent*, pp. 31–37.
- Okal, B., Arras, K.O., 2016a. Formalizing normative robot behavior. 8th International Conference, on Social Robotics, in: *Proc. International Conference on Social Robotics (ICSR'16)*, Kansas, USA. pp. 62–71.
- Okal, B., Arras, K.O., 2016b. Learning socially normative robot navigation behaviors with bayesian inverse reinforcement learning, in: *Robotics and Automation (ICRA), 2016 IEEE International Conference on*, IEEE. pp. 2889–2895.
- Olson, E., Leonard, J., Teller, S., 2006. Fast iterative alignment of pose graphs with poor initial estimates, in: *Robotics and Automation, 2006. ICRA 2006. Proceedings 2006 IEEE International Conference on*, IEEE. pp. 2262–2269.
- Papadakis, P., Rives, P., Spalanzani, A., 2014. Adaptive spacing in human-robot interactions, in: *Intelligent Robots and Systems (IROS 2014), 2014 IEEE/RSJ International Conference on*, IEEE. pp. 2627–2632.
- Papadakis, P., Spalanzani, A., Laugier, C., 2013. Social mapping of human-populated environments by implicit function learning, in: *Intelligent robots and systems (IROS), 2013 IEEE/RSJ international conference on*, IEEE. pp. 1701–1706.
- Pérez-Higueras, N., Caballero, F., Merino, L., 2016. Learning robot navigation behaviors by demonstration using a rrt* planner, in: *International Conference on Social Robotics*, Springer. pp. 1–10.
- Ratsamee, P., Mae, Y., Ohara, K., Kojima, M., Arai, T., 2013. Social navigation model based on human intention analysis using face orientation, in: *Intelligent Robots and Systems (IROS), 2013 IEEE/RSJ International Conference on*, IEEE. pp. 1682–1687.
- Rios-Martinez, J., Spalanzani, A., Laugier, C., 2015. From proxemics theory to socially-aware navigation: A survey. *International Journal of Social Robotics* 7, 137–153.
- Rios-Martinez, J.A., 2013. *Socially-Aware Robot Navigation: combining Risk Assessment and Social Conventions*. Hal.Inria.Fr .
- Scandolo, L., Fraichard, T., 2011. An anthropomorphic navigation scheme for dynamic scenarios, in: *Robotics and Automation (ICRA), 2011 IEEE International Conference on*, IEEE. pp. 809–814.
- Sisbot, E.A., Marin-Urias, L.F., Alami, R., Simeon, T., 2007. A human aware mobile robot motion planner, IEEE. pp. 874–883.
- Sutcliffe, A., Pineau, J., Tenenholz, N., 2015. Missteps in robot social navigation, in: *AAAI 2015 Fall Symposium on Artificial Intelligence for Human-Robot Interaction*, AAAI. pp. 134–136.
- Svenstrup, M., Tranberg, S., Andersen, H.J., Bak, T., 2009. Pose estimation and adaptive robot behaviour for human-robot interaction, in: *Robotics and Automation, 2009. ICRA'09. IEEE International Conference on*, IEEE. pp. 3571–3576.
- Takayama, L., Pantofaru, C., 2009. Influences on proxemic behaviors in human-robot interaction, in: *Intelligent robots and systems, 2009. IROS 2009. IEEE/RSJ international conference on*, IEEE. pp. 5495–5502.
- Tipaldi, G.D., Arras, K.O., 2011a. Planning Problems for Social Robots, in: *Proc. International Conference on Automated Planning and Scheduling (ICAPS'11)*, Freiburg, Germany.
- Tipaldi, G.D., Arras, K.O., 2011b. Please do not disturb! minimum interference coverage for social robots, in: *Proc. IEEE/RSJ International Conference on Intelligent Robots and Systems (IROS'11)*, San Francisco, USA. pp. 1968–1973.
- Vega, A., Manso, L., Macharet, D., Bustos, P., Núñez, P., 2017a. A new Strategy based on an Adaptive Spatial Density Function for Social Robot Navigation in Human-Populated Environments., in: *Proceedings of REACTS workshop at the International Conference on Computer Analysis and Patterns*.
- Vega, A., Manso, L.J., Bustos, P., Núñez, P., Macharet, D.G., 2017b. Socially acceptable robot navigation over groups of people, in: *IEEE Conference on Robot and Human Interactive Communication, RO-MAN2017*, Portugal.
- Vieira, A.W., Drews, P.L., Campos, M.F., 2014. Spatial density patterns for efficient change detection in 3d environment for autonomous surveillance robots. *Ieee Transactions on Automation Science and Engineering* 11, 766–774.
- Walters, M.L., Oskoei, M.A., Syrdal, D.S., Dautenhahn, K., 2011. A long-term human-robot proxemic study, in: *RO-MAN, 2011 IEEE*, IEEE. pp. 137–142.